Preprints (www.preprints.org) | NOT PEER-REVIEWED | Posted: 31 December 2018 doi:10.20944/preprints201812.0359.v1

Peer-reviewed version available at Metals 2019, 9, 301; doi:10.3390/met9030301

Article

Mechanical Behavior of Inconel 625 at Elevated Temperatures

Mauro M. de Oliveira [1], Antônio A. Couto [1,2], Gisele F. C. Almeida [1, 2,*], Danieli A. P. Reis [3,4], Nelson B. de Lima[1] and Renato Baldan [5,*]

[1] Center for Materials Science and Technology, Instituto de Pesquisas Energéticas e Nucleares, São Paulo, Brazil; mauromach@gmail.com (M.M.O); acouto@ipen.br (A.A.C.); nblima@ipen.br (N.B.L.)
[2] Department of Materials Engineering and Nanotechnology, Universidade Presbiteriana Mackenzie, São Paulo, Brazil; acouto@ipen.br (A.A.C.); gisele_fab@hotmail.com (G.F.C.A)
[3] Science and Technology Department, Universidade Federal de São Paulo—UNIFESP, São José dos Campos, Brazil; danielireis@gmail.com (D.A.P.R.)
[4] Department of Aeronautical and Mechanical Engineering, Instituto Tecnológico de Aeronáutica – ITA/DCTA, São José dos Campos, Brazil.; danielireis@gmail.com (D.A.P.R.)
[5] Department of Production Engineering, Universidade Estadual Paulista – UNESP, Itapeva, Brazil; renato@itapeva.unesp.br
* Correspondence: gisele_fab@hotmail.com; Tel.: +55-119-9639-8967

Abstract: The Inconel 625 is a nickel-based alloy has been widely used in the high-temperature application. The Inconel 625 exhibits unstable plastic flow at elevated temperature characterized by serrated yielding, known as Portevin-Le Chatelier effect. The aim of this work is to evaluate the mechanical properties at high temperatures of the Inconel 625. The tensile tests were performed in the temperature range of room temperature until 1000 °C and strain rate of $2x10^{-4}$ to $2x10^{-3}$ s^{-1}. The creep tests were performed in the temperature range of 600-700 °C, in the stress range of 500-600 MPa in a constant load mode. The surface fracture was observed by optical and scanning electron microscopy. Serrated stress-strain behavior was observed in the curves obtained at 200 to 700°C, which was associated with the dynamic strain aging effect. The yield strength and the elongation values show an anomalous behavior as a function of the test temperature. An intergranular cracking was observed specimen tensile tested at 500 °C that can be attributed to the decohesion of the carbides along the grain boundaries. The fracture surface of the specimen tensile tested at 700 °C showed the predominance of transgranular cracking with tear dimples with a parabolic shape.

Keywords: Inconel; high temperature; tensile test; creep; serrated; dynamic strain aging

1. Introduction

The Inconel 625 is a nickel-based alloy has been widely used in the high temperature application such as aerospace, petrochemical, marine and nuclear industries because of its excellent oxidation resistance and superior mechanical properties [1–3]. This superalloy is strengthened by the solid-solution-hardening effects of chromium, molybdenum, niobium, and iron and precipitation-hardening effects of the intermetallic phases [1].

The Inconel 625 exhibits unstable plastic flow at elevated temperature characterized by serrated yielding, known as Portevin-Le Chatelier (PLC) effect. This phenomenon is usually attributed to the dynamic strain ageing (DSA) [4–6]. The PLC effect is observed in many nickel-based superalloys within a certain range of deformation temperature and strain rate [7]. This phenomenon has a significant effect on the mechanical properties of this material. The dynamic interaction between mobile dislocation and diffusion solute atoms during plastic deformation is a commonly accepted explanation of this phenomenon.

The purpose of this work was investigated the mechanical behavior of Inconel 625 superalloy at elevated temperatures. The tensile tests were performed in the temperature range of room temperature until 1000 °C and strain rate of $2x10^{-4}$ to $2x10^{-3}$ s^{-1}. The creep tests were performed in the

© 2018 by the author(s). Distributed under a Creative Commons CC BY license.

Preprints (www.preprints.org) | NOT PEER-REVIEWED | Posted: 31 December 2018 doi:10.20944/preprints201812.0359.v1

Peer-reviewed version available at Metals 2019, 9, 301; doi:10.3390/met9030301

temperature range of 600-700 °C, in the stress range of 500-600 MPa in a constant load mode. The serrated flow behavior was examined, the activation energy for DSA was evaluated, and the mechanical properties were correlated with the fracture modes.

2. Materials and Methods

The Inconel 625 alloy was received in cylindrical bars with diameter of 12 mm, hot forging. The chemical composition of the main elements (percentage by weight) meets the ASTM B443-00 requirements [8], as shown in Table 1. The inductively coupled plasma optical emission spectrometry (ICP-OES) analysis was performed in an ARL equipment 3410 model (Laboratory of Analytical Chemistry of the Department of Materials Engineering, School of Engineering of Lorena - EEL - USP, Lorena, Brazil) to verify the chemical composition of the material.

Table 1. Chemical composition required for Inconel 625 alloy.

Element	Ni	Cr	Mo	Nb+Ta	Fe	Mn	Si	Ti	Al	C
wt %	Min. 58.0	20.0-23.0	8.0/10.0	3.15-4.15	Max. 5.0	Max. 0.5	Max. 0.5	Max. 0.4	Max. 0.4	Max. 0.1

For microstructural characterization the samples were prepared by a standard grinding procedure using silicon carbide papers, polished with alumina solution and diamond paste, and electrolytic etched in a 10% oxalic acid solution and current density of 100 mA/cm^2.

The tensile tests were performed at room temperature up to 1000 °C in an Universal Testing Instrument (model 4400R, Instron, São José dos Pinhais, Brazil). The specimens had a diameter of 6 mm and reduced section of 30 mm. Two type K thermocouple (Minnesota Measurement Instruments LLC, Minnesota, USA) leaning against the reduced section was used to control the temperature. The strain rates used were $2x10^{-4}$ to $2x10^{-3}$ s^{-1}. The specimens were held at test temperature for 30 minutes before the traverse movement start. In the tensile test were determined the yield strength at a strain offset of 0.002 (YS), the tensile strength (TS) and the elongation (EL) from the engineering stress–strain curve.

The creep tests were performed according to ASTM E-139-11 [9] in a furnace adapted with electrical systems and controllers (Denison Mayes Group, Leeds, UK). A linear variable differential displacement transducer (LVDT, Denison Mayes Group, Leeds, UK) was used to obtain measures of elongation, and a Cromel / Alumel type K thermocouple was used to control the temperature. The tests were performed at 600, 650, and 700 °C at 500, 550, and 600 MPa in a constant load mode.

After the tensile and creep tests the fracture surfaces of the specimens were examined using a Scanning Electron Microscope (SEM) (JSM-6510, JEOL Ltd., Tokyo, Japan) in order to determine the predominant fracture mode. For microstructural observation some crept samples were longitudinally sectioned along the mid-plane close to the fracture plane.

3. Results and Discussion

3.1. Material Characterization

The results obtained by the ICP-OES are summarized in Table 2 and the chemical composition was adequate of the ASTM requirements (B443-00) [8].

Table 2. Chemical composition of Inconel 625 alloy obtained by the ICP-OES.

Element	Ni	Cr	Mo	Nb	Fe	Mn	Ti	Al	C
wt %	balance	21.5	9.4	3.6	2.5	0.25	0.27	0.29	0.05

The microstructural analysis showed an austenitic microstructure formed by equiaxial grains in the transversal and longitudinal direction of the bar with an ASTM E112 [10] grain size of 11, as shown in Figure 1.

Preprints (www.preprints.org) | NOT PEER-REVIEWED | Posted: 31 December 2018 doi:10.20944/preprints201812.0359.v1

Peer-reviewed version available at Metals 2019, 9, 301; doi:10.3390/met9030301

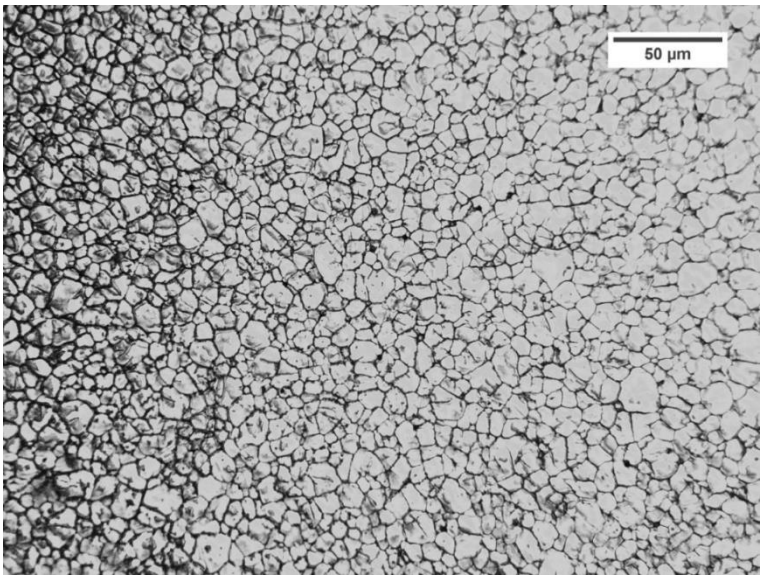

Figure 1. Optical micrograph of the longitudinal section of the bar of Inconel 625.

3.2. Tensile tests

The Inconel 625 tensile tests were performed at a strain rate of 2 X 10^{-4} s^{-1} in the temperature range of 25 °C (room temperature) to 1000 °C. The tests results are summarized in Table 3, including 0.2% yield strength (YS), ultimate tensile stress (UTS) and elongation (EL). The tensile data were plotted in Figure 2. The yield strength values show an anomalous behavior as a function of the temperature. From the room temperature until around 600 °C, occurs a decrease in the yield strength and a slight increase up to 700 ° C, decreasing sharply at temperatures above 700 ° C. In relation to the elongation, there is an increasing tendency with the test temperature increase. An anomaly is also present in this case, at temperatures close to 600 °C occurs a significant decrease in the elongation.

Table 3. Mechanical properties of Inconel 625 alloy obtained by the tensile tests at room temperature until 1000 °C.

Test temperature (°C)	YS (MPa)	UTS (MPa)	EL (%)
23	598	971	40
200	556	940	53
400	434	845	67
500	473	829	61
600	444	807	34
700	484	722	67
800	392	403	61
900	195	199	61
1,000	98	104	78

This anomalous behavior in the tensile properties at temperatures close to 600 °C in was also evidenced by other authors [4,5,11–18] and it depends on the strain rate applied in the test. According to these researches, at a strain rate less than 10^{-5} s^{-1}, this anomalous behavior is no longer observed, resulting in a continuous drop in the yield strength and a continuous ductility increase with the tensile test temperature increase. Concerning the ultimate strength, a slight decrease occurs up to the test temperature of 600 °C and a sharp decrease in this property for temperatures above 700 °C. At 600 °C, in addition to the strain rate of 2 X 10^{-4} s^{-1}, tensile tests were also performed at 1 X 10^{-3} s^{-1} and 2 X 10^{-3} s^{-1}. There were no significant differences in the mechanical properties results due to

Preprints (www.preprints.org) | NOT PEER-REVIEWED | Posted: 31 December 2018 doi:10.20944/preprints201812.0359.v1

Peer-reviewed version available at Metals 2019, 9, 301; doi:10.3390/met9030301

the variation of the strain rates applied. However, smaller strain rates were not tested nor was the strain rate variation tested at other temperatures, making it impossible to compare the work of the authors mentioned above [4,5,11–18].

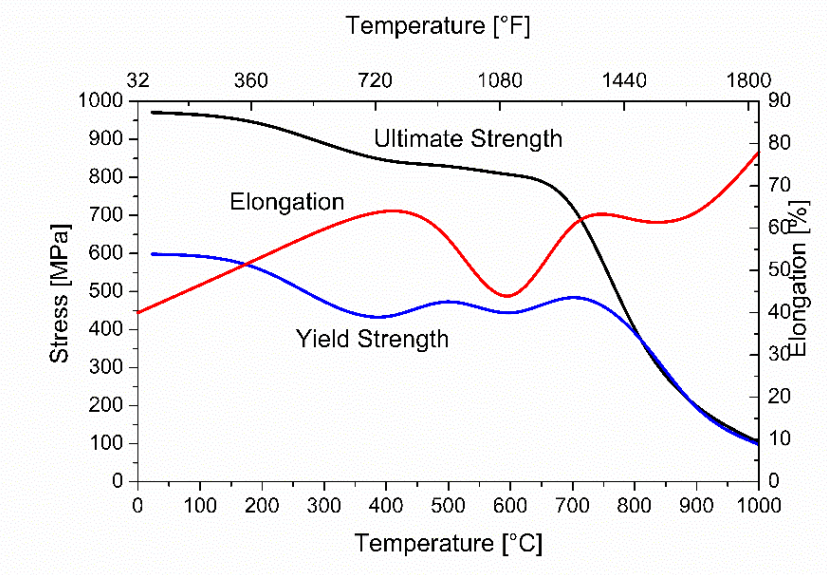

Figure 2. Yield stress, ultimate tensile stress, and elongation obtained from Inconel 625 tensile tests as a function of the test temperature.

The stress-strain curves obtained in the tensile tests at room temperature up to 1000 °C are shown in Figure 3. In the tensile tests performed at temperatures between 200 and 700 °C it was possible to observe a serrated curve in the region of plastic deformation in the stress-strain curves, this phenomenon is already observed in numerous works on nickel alloys [12,17]. Serrations are defined as repeated and systematic fluctuations of the stress during the strain [19]. This type of plastic instability manifested in many metals is called the Portevin-Le Chatelier (PLC) effect [20]. The most accepted mechanism for the formation of the serrated is the dynamic strain aging (DSA) during the plastic deformation as result of the interaction between solute atoms and mobile dislocations [7,19]. Each stress drop matches to the formation of a band and is accompanied by an audible acoustic emission [15]. In the tensile tests at 700 °C the serrated occurred only in the initial region of plastic deformation in the stress-strain curve. While in the tests above 800 °C this serrated-flow behavior was not observed.

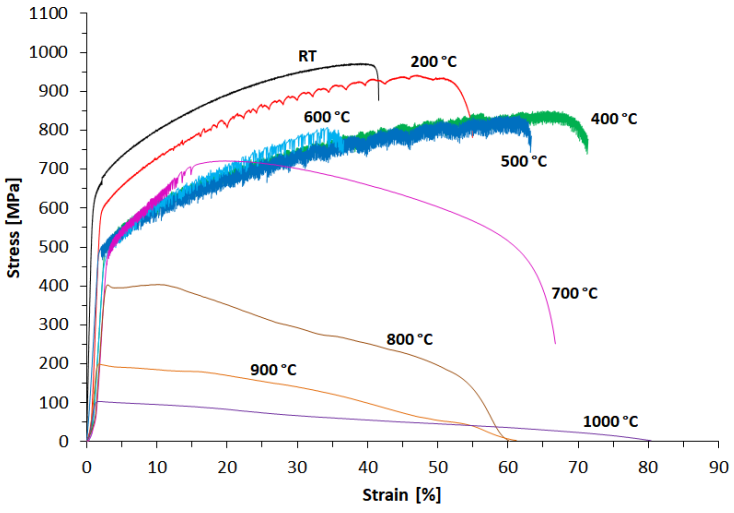

Figure 3. Stress-strain curves obtained from Inconel 625 tensile tests at room temperature (RT) until 1000 °C.

Preprints (www.preprints.org) | NOT PEER-REVIEWED | Posted: 31 December 2018 doi:10.20944/preprints201812.0359.v1

Peer-reviewed version available at Metals 2019, 9, 301; doi:10.3390/met9030301

Hale et al [12] have associated the serration flow behavior in Ni-based superalloys to the diffusion of an interstitial solute, such as carbon at lower temperatures and the diffusion of substitutional atoms, such as molybdenum and chromium at higher temperatures [4,21]. The dislocation-solute atom interaction model used by many researchers is the theory about the interaction between mobile dislocations and diffusing solute atoms, first suggested by Cottrell [20] and followed by several authors [22–33]. The type of serration depends on the strain rate and the temperature [1]. The serrations were identified as types A, B and C according to the classification scheme [34,35] shown in Figure 4. The serrations appear to occur randomly but from a more detailed inspection, it can be noted that they form distinguishable patterns which, under specific conditions, show certain regularity [7]. The A-type serrations are observed at high strain rates and low temperatures. The B-type serrations occur at medium to high strain rates and appear in correlated bands. The C-type serrations are observed at low strain rates and high temperatures and are more regular [7,12,19].

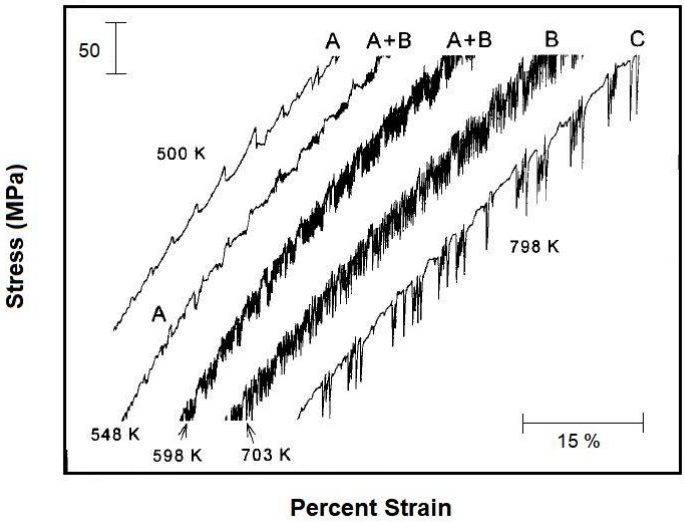

Figure 4. Various types of serrated flow observed in the stress–strain curves of Inconel 718 (adapted from Hale et al. [12])

Details of the plastic strain region of the stress-strain curves obtained in the tensile tests at room temperature, 200, 300 e 500 °C are shown in Figure 5. Note that even at room temperature, a slight oscillation in stress occurs. However, with a much smaller amplitude when compared to the serrated observed on the test at 500 ° C. The stress-strain curve at 200 °C showed an A-type serrated, while at the 500 °C it was observed B-type serrated. This B-type serrated occurred in the test temperature range between 400 and 700 °C. In the tensile tests at 300 °C, a transition appears to occur, with serrated A+B-type. The predominance of A and B-type serrated in the tensile test curves at low temperatures and high strain rates are consistent with previous work [7,12,17–19]. A and B-type serrated are related to the diffusion of C atoms in Ni-based alloys [12]. The C-type serrated was not observed in the stress-strain curves, it should only appear in tests at high temperatures and low strain rates that were not used in this work.

Figure 6 shows stress-strain curves obtained in tensile tests at 600 °C and strain rates of 2 X 10^{-4}, 1 X 10^{-3} and 2 X 10^{-3} s^{-1}. Higher strain rates induced a lower frequency and higher amplitude. The lower strain rate results in a longer time for the dislocations to overcome the obstacles. Therefore, the serrations magnitude is increased, resulting in the change in the serrations type. The strain rate sensitivity (m) was determined in tensile tests at the same temperature and at varying strain rates. The stress corresponding to 5% of plastic strain in the tensile tests at a temperature of 600 °C was adopted for the determination of the strain rate sensitivity. The strain rate sensitivity was obtained using the following expression:

Preprints (www.preprints.org) | NOT PEER-REVIEWED | Posted: 31 December 2018 doi:10.20944/preprints201812.0359.v1

Peer-reviewed version available at Metals 2019, 9, 301; doi:10.3390/met9030301

$$m = \log(\sigma_2/\sigma_1)/\log(\dot{\varepsilon}_2/\dot{\varepsilon}_1) \quad (1)$$

The strain rate sensitivity obtained, m, was -0.02. The value is similar as that obtained by Nagesha [21]. The PLC effect occurs when the strain rate sensitivity becomes negative and is associated with the manifestation of plastic instabilities in the uniaxial deformation [5,7,12,15,21].

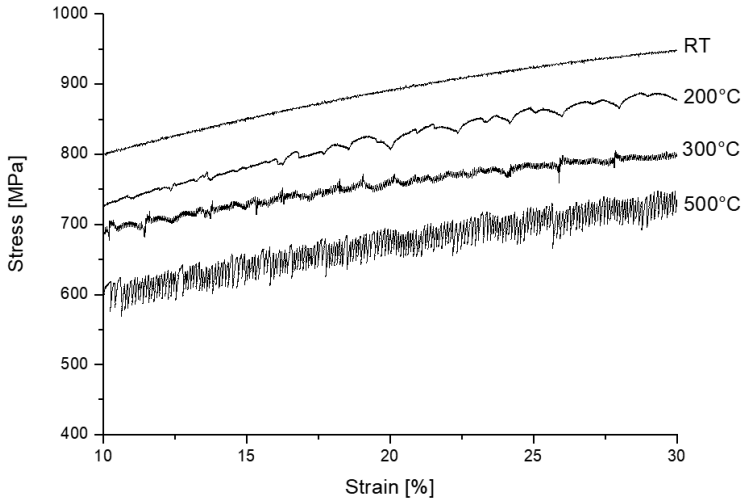

Figure 5. Details of the plastic strain region of the stress-strain curves obtained in the Inconel 625 tensile tests at room temperature, 200, 300 e 500 °C.

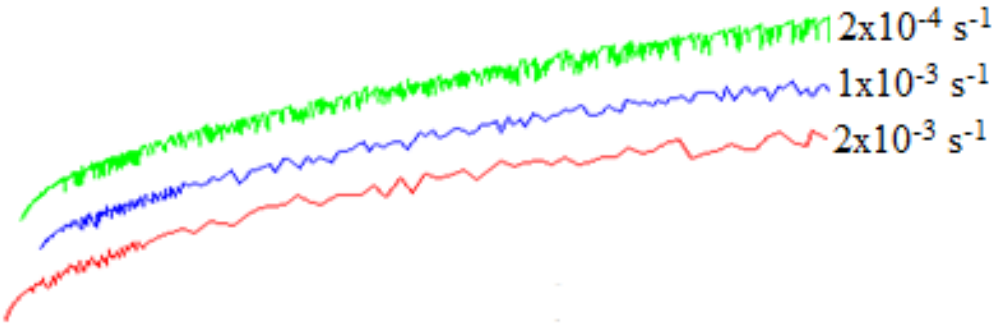

Figure 6. Details of the stress-strain curves obtained in the Inconel 625 tensile tests at 600 °C varying the strain rate.

Longitudinal sections of tensile fracture for the specimens tested at (a) 500 and (b) 800 °C in low magnification micrographs are shown in Figure 7. In the specimen tested at 500 °C can be noted that the fracture occurred in a macroscopic plane inclined 45° to the tensile axis. This fracture type occurred systematically in all specimens in which the Portevin-Le Chatelier (PLC) effect was observed on the stress-strain curve, which led to plastic instabilities (serrated) in plastic strain until the fracture. In tensile tests at temperatures above 700 °C the PLC effect no longer occurred, and the specimens also no longer ruptured at 45° to the tensile axis, as can be seen in the Figure 6(b). This particular mode of failure by extensive shearing on a macroscopic plane inclined 45° to the tensile axis had already been observed by Fournier et al [15].

Preprints (www.preprints.org) | NOT PEER-REVIEWED | Posted: 31 December 2018 doi:10.20944/preprints201812.0359.v1

Peer-reviewed version available at Metals 2019, 9, 301; doi:10.3390/met9030301

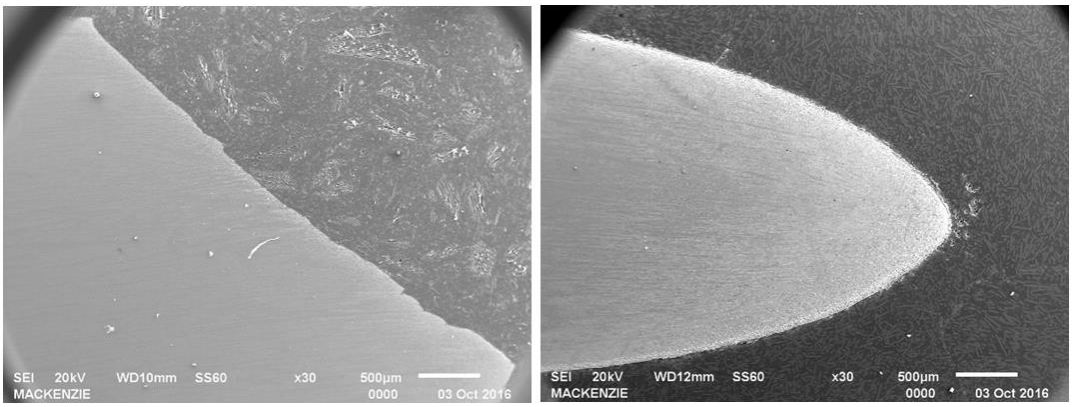

Figure 7. Micrographs of the longitudinal sections of tensile fracture for the Inconel 625 specimens tested at (a) 500 and (b) 800 °C.

A detail of the longitudinal section of the fracture region of the specimen tensile tested at 500 °C is shown in Figure 8 (a). In this figure, an intergranular cracking is observed that can be attributed to the precipitation of carbides at grain boundaries. The decohesion of the carbides along the grain boundaries is responsible for the crack nucleation [15]. The fracture surface of this specimen is shown in Figure 8 (b), with the arrow indicating the intergranular cracking. Grain boundaries cracks were extensively observed throughout the fracture surface in specimens tested at this temperature. However, in this fractography is also observed the formation of cavities on the entire fracture surface, typical of ductile fracture. Shankar and Han [1,4] also observed similar fracture surfaces in tensile test specimens at these temperatures.

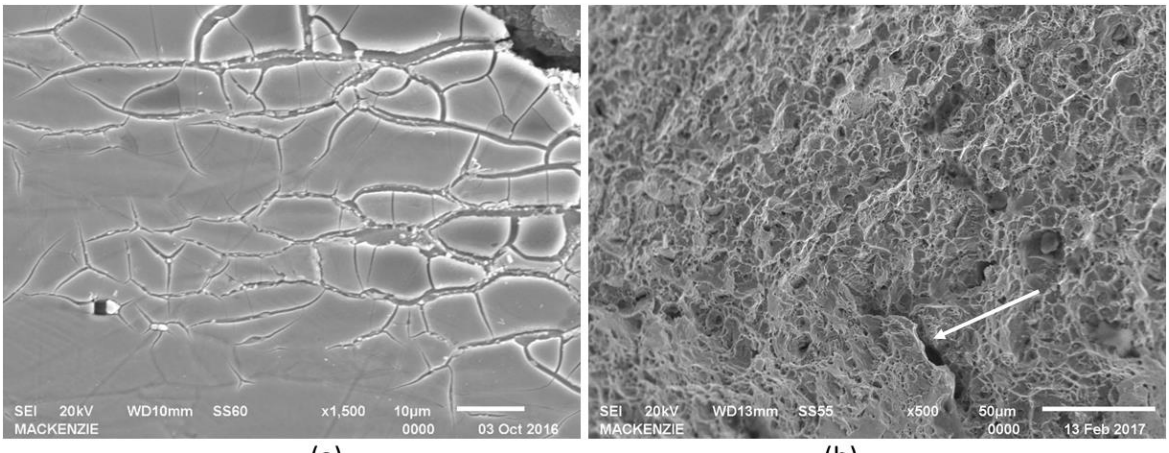

Figure 8. Micrographs of (a) the detail of the longitudinal section of the Inconel 625 fracture region tensile tested at 500 °C and (b) fracture surface of this specimen with the arrow indicating intergranular cracking.

Figure 9 shows the micrographs of the region close to the fracture of the specimens tensile tested at (a) 600 °C and at (b) 700 °C. A grain size not considerable modified is noticeable in these micrographs, but with an elongation in the tensile direction as indicated by the arrows. More elongated grains are observed in the specimen tested at 700 °C.

Preprints (www.preprints.org) | NOT PEER-REVIEWED | Posted: 31 December 2018 doi:10.20944/preprints201812.0359.v1

Peer-reviewed version available at Metals 2019, 9, 301; doi:10.3390/met9030301

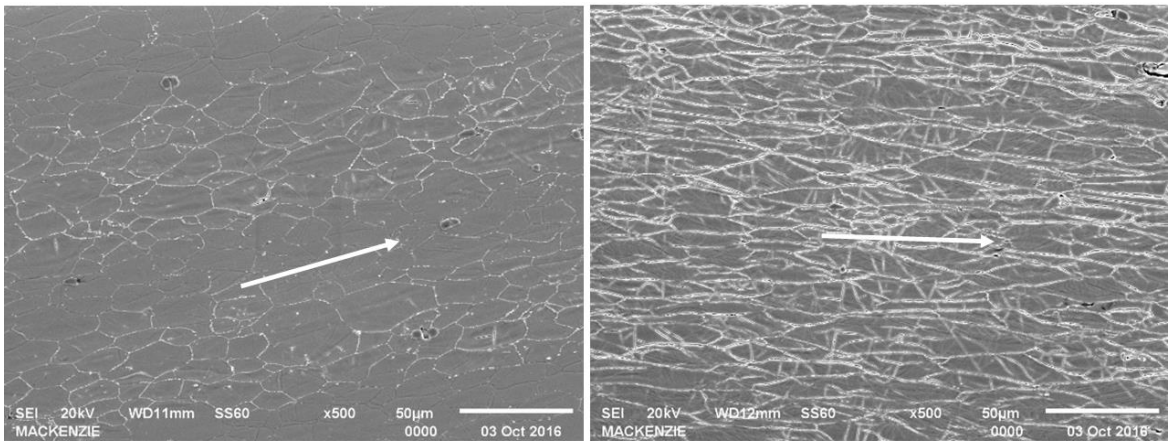

Figure 9. Micrographs of the region close to the fracture of the Inconel 625 specimens tensile tested at (a) 600 °C and at (b) 700 °C. The arrows are indicating the tensile test direction.

The typical fracture surface of the tensile test specimen at these temperatures is shown in Figure 10 (a). Slip bands are observed in the region in evidence, also seen by Hrutkay [11]. In Figure 10 (b) several slip lines can be seen inside the grains. The slip bands are formed during the plastic strain when strain-hardening occurs and may be responsible for a lower ductility. Note also the presence of carbides along the grain boundaries in both conditions [4]. The fracture surface of the specimen tensile tested at 700 °C is shown in Figure 11. Note the predominance of transgranular cracking with tear dimples with parabolic shape.

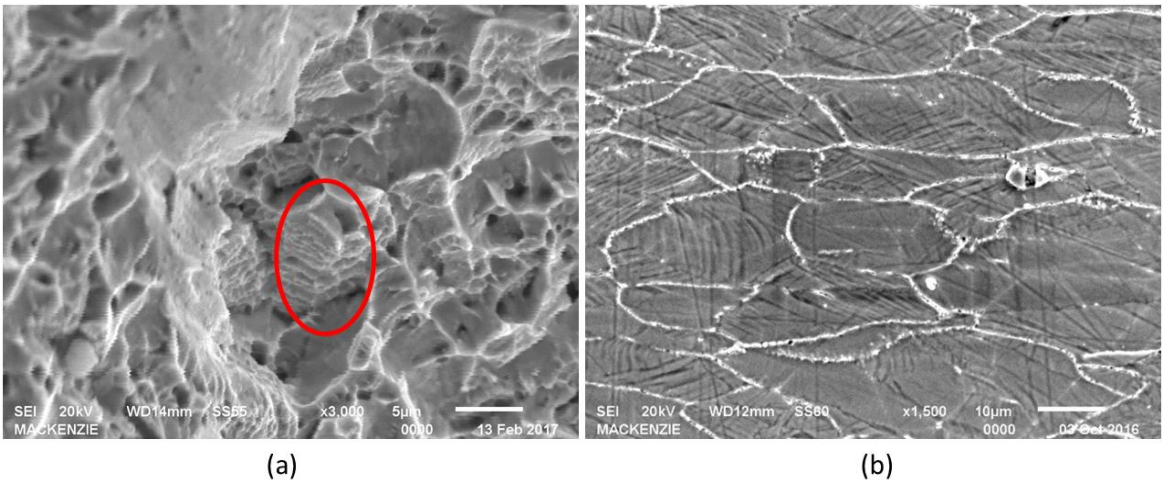

Figure 10. Micrographs of the Inconel 625 tensile tested at 700 °C: (a) typical fracture surface with slip bands in evidence and (b) longitudinal section of fracture region.

The longitudinal section of the fracture region of a specimen tensile tested at 800 °C is shown in Figure 12. In this figure is observed the presence of equiaxial smaller grains, probably derived from the dynamic recrystallization. It was not possible to observe the presence of carbides in the grain boundaries. The similar microstructure was observed in the specimens tested at 900 and 1000 °C. The fracture surfaces of specimens tested at temperatures above 700 °C could not be analyzed due to the practically nonexistent fracture area, as shown in Figure 7 (b).

Preprints (www.preprints.org) | NOT PEER-REVIEWED | Posted: 31 December 2018 doi:10.20944/preprints201812.0359.v1

Peer-reviewed version available at Metals 2019, 9, 301; doi:10.3390/met9030301

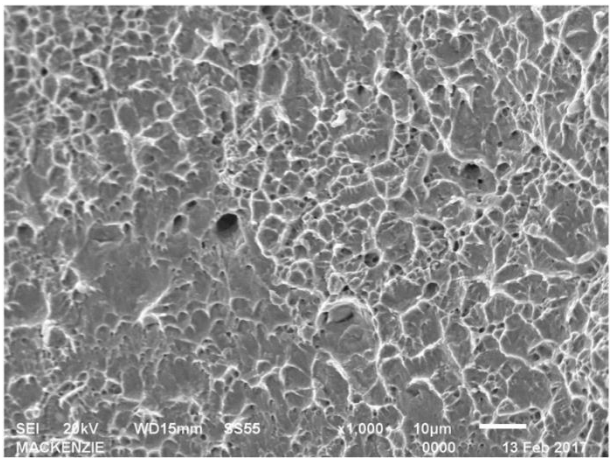

Figure 11. Micrographs of the Inconel 625 fracture surface tensile tested at 700 °C showing transgranular cracking with tear dimples.

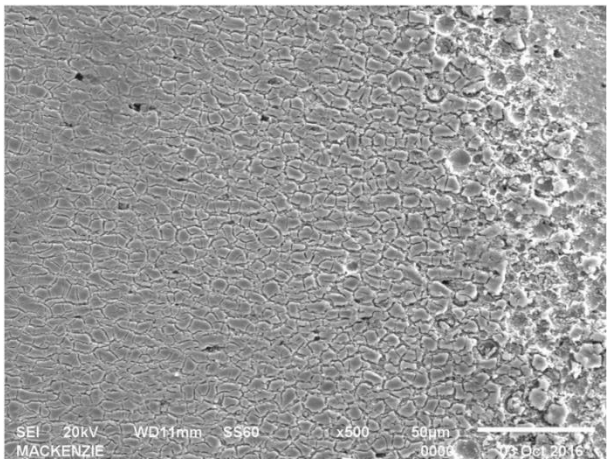

Figure 12. Micrograph of the longitudinal section of the Inconel 625 fracture region tensile tested at 800 °C showing equiaxial grains.

3.3. Creep tests

The creep tests were performed in the Inconel 625 specimens. The results of the short-term creep tests performed under constant load are summarized in Table 4, where they were being presented the primary creep time (*tp*), the and secondary creep rate ($\dot{\varepsilon}_s$). Due to the long time to reach the fracture of this material the tests were interrupted at determined times for each condition of temperature and stress.

Table 4. Creep data of the Inconel 625.

Temperature (°C)	σ (MPa)	*tp* (h)	$\dot{\varepsilon}_s$ (1/h)
600	500	235.5	1.78×10^{-6}
650	500	23.6	1.32×10^{-4}
	550	12.5	3.74×10^{-4}
	600	10.0	1.13×10^{-3}
700	500	17.1	5.39×10^{-4}

The creep curve obtained at 650 °C and 500 MPa, corresponding to true strain ε as a function of the time *t*, is shown in Figure 13. This test was interrupted after 75 hours without breaking. From the tests results was calculated the stress exponent (*n*) and the creep activation energy (*Qc*). Figure 14

Preprints (www.preprints.org) | NOT PEER-REVIEWED | Posted: 31 December 2018 doi:10.20944/preprints201812.0359.v1

Peer-reviewed version available at Metals 2019, 9, 301; doi:10.3390/met9030301

shows the curve logarithmic relationship between steady creep rates and stress at 650 °C of the Inconel 625 alloy. The value of the stress dependence of the steady-state creep rate (n) can be described in terms of power-law creep equations using standard regression techniques [36]:

$$\dot{\varepsilon}_s = B\,\sigma^n \quad (1)$$

where B is the structure-dependent constant and σ is the applied stress.

The Figure 15 shows the curve logarithmic relationship between steady creep rates and inverted absolute temperature at 500 MPa. The values of the creep activation energy (Qc) can be described in terms of the Arrhenius's Law by standard regression techniques [36]:

$$\dot{\varepsilon}_s = B_0\,\sigma^n exp(-Q_c/RT) \quad (2)$$

where B_0 is the structure-dependent constant, σ is the applied stress, R is the gas constant, and T is the temperature that is applied.

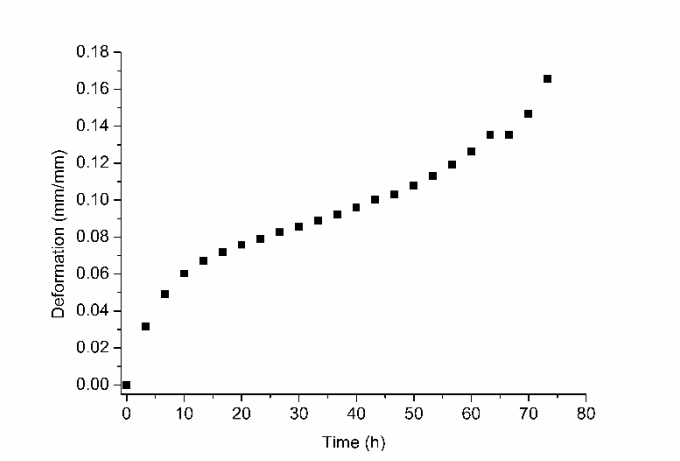

Figure 13. Creep curve of the Inconel 625 alloy at 650 °C and 600 MPa.

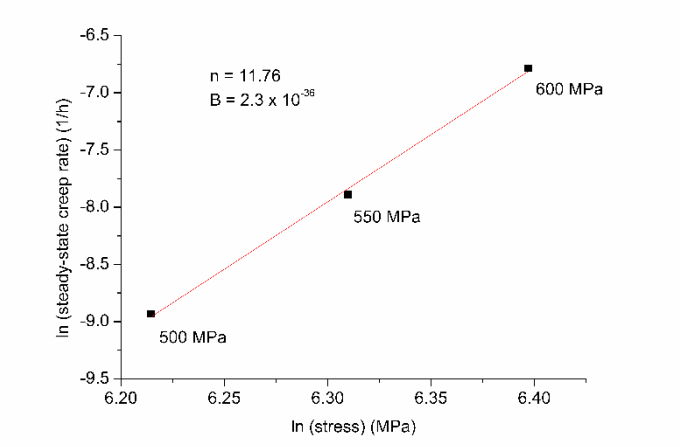

Figure 14. Steady-state creep rate dependence with the stress applied at 650 °C of Inconel 625 alloy.

Preprints (www.preprints.org) | NOT PEER-REVIEWED | Posted: 31 December 2018 doi:10.20944/preprints201812.0359.v1

Peer-reviewed version available at Metals 2019, 9, 301; doi:10.3390/met9030301

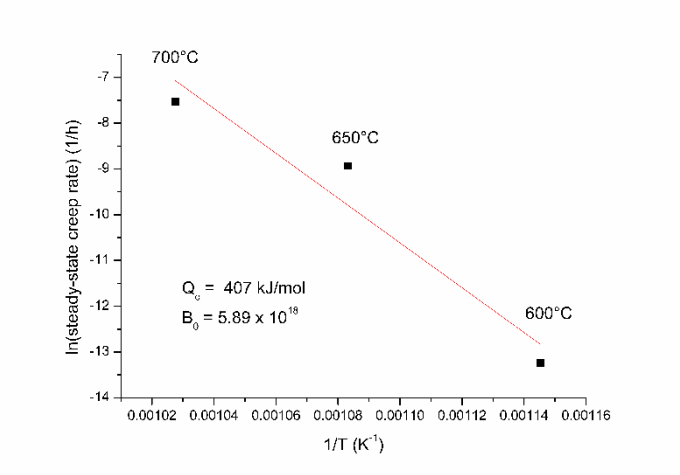

Figure 15. The diagram to determine the activation energy (*Qc*) at 500 MPa of the Inconel 625 alloy.

The value of core diffusion activation energy ($Q_{(core)}$) for Nickel reported from Frost and Ashby [37] was 170 kJ/mol. Moore et al [38] found different values of self-diffusion activation energy for the Inconel 625 alloy according to the temperature. The value of the activation energy obtained for Moore et al [38] was 108.3 ± 6.6 kJ/mol above 700 °C and 46.6 ± 12.2 kJ/mol below 650 °C. Between 650-700 °C, a significantly higher value of the activation energy of 527.7 ± 23.1 kJ/mol was found. This result was attributed ultimately a consequence of a high driving force, solute-impeded grain boundary migration process operating within the alloy. The activation energy value found in this work was 407 kJ/mol. This higher value obtained at the same temperature as Moore et al [38] may be related to the DSA effect present in Inconel 625.

For tests performed at temperatures between 40 to 70% of the melting point (1290-1350°C) under intermediate or high stress levels, the n values larger than three and the activation energy for creep (Qc) values near core diffusion activation energy ($Q_{(core)}$) suggest that the dominant mechanism is dislocation creep according to Evans and Wilshire [36]. The values of n = 11.76 and Qc = 407 kJ/mol found in this work agree with these conditions.

In order to understand the effect mechanism of the PLC, several methods can be employed to calculate the activation energy of the serrated flow [4,12]. The amount of activation energy can vary greatly depending on the method used to evaluate it. Moreover, these values are altered with the strain rate and temperature, which could notably influence the activation energy for the serrated flow. Therefore, it is difficult to make any association related to these values.

5. Conclusions

The study of the mechanical behavior of Inconel 625 at elevated temperatures allowed concluding that:

- The yield strength values show an anomalous behavior as a function of the temperature. From the room temperature until around 600 °C, occurs a decrease in the yield strength and a slight increase up to 700 °C, decreasing sharply at temperatures above 700 °C. In relation to the elongation, an anomaly is also present, with a significant decrease in the elongation at temperatures close to 600 °C.
- In the tensile tests performed at temperatures between 200 and 700 °C, it was possible to observe a serrated curve in the region of plastic deformation in the stress-strain curves. The stress-strain curve at 200 °C showed an A-type serrated, while in the test temperature range between 400 and 700 °C it was observed B-type serrated. In the tensile tests at 300 °C, a transition appears to occur, with serrated A+B-type.
- In all specimens in which the Portevin-Le Chatelier effect was observed on the stress-strain curve (serrated), can be noted that the fracture occurred in a macroscopic plane inclined 45° to the tensile axis.

Preprints (www.preprints.org) | NOT PEER-REVIEWED | Posted: 31 December 2018 doi:10.20944/preprints201812.0359.v1

Peer-reviewed version available at Metals 2019, 9, 301; doi:10.3390/met9030301

- An intergranular cracking was observed specimen tensile tested at 500 °C that can be attributed to the decohesion of the carbides along the grain boundaries. The fracture surface of the specimen tensile tested at 700 °C showed the predominance of transgranular cracking with tear dimples with parabolic shape. Several slip lines can be seen inside the grains and the presence of carbides along the grain boundaries.
- The values of n = 11.76 and Qc = 407 kJ/mol found in this work suggest that the dominant mechanism is dislocation creep. This significantly higher value of the activation energy was attributed ultimately a consequence of a high driving force, solute-impeded grain boundary migration process operating within the alloy and may be related to the DSA effect present in Inconel 625.

Preprints (www.preprints.org) | NOT PEER-REVIEWED | Posted: 31 December 2018 doi:10.20944/preprints201812.0359.v1

Peer-reviewed version available at Metals 2019, 9, 301; doi:10.3390/met9030301

Author Contributions: Conceptualization: M.M.O., A.A.C. and R.B.; Formal analysis: M.M.O., D.A.P.R. and N.B.L.; Investigation: M.M.O., A.A.C., G.F.C.A. and R.B.; Supervision, A.A.C.; Validation: G.F.C.A., D.A.P.R., N.B.L. and R.B.; Writing – original draft: A.A.C.; Writing – review & editing: G.F.C.A.

Funding: This research received no external funding.

Conflicts of Interest: The authors declare no conflict of interest.

References

1. Shankar, V.; Valsan, M.; Rao, K.B.S.; Mannan, S.L. Effects of temperature and strain rate on tensile properties and activation energy for dynamic strain aging in alloy 625. *Metall. Mater. Trans. A Phys. Metall. Mater. Sci.* **2004**, *35 A*, 3129–3139.

2. Korrapati, P.K.; Avasarala, V.K.; Bhushan, M.; Ramkumar, K.D.; Arivazhagan, N.N.; Narayanan, S. Assessment of Mechanical Properties of PCGTA Weldments of Inconel 625. *Procedia Eng.* **2014**, *75*, 9–13.

3. Dokme, F.; Kulekci, M.; Esme, U.; Dokme, F.; Kulekci, M.K.; Esme, U. Microstructural and Mechanical Characterization of Dissimilar Metal Welding of Inconel 625 and AISI 316L. *Metals (Basel).* **2018**, *8*, 797.

4. Han, F.F.; Zhou, B.M.; Huang, H.F.; Leng, B.; Lu, Y.L.; Dong, J.S.; Li, Z.J.; Zhou, X.T. The tensile behavior of GH3535 superalloy at elevated temperature. *Mater. Chem. Phys.* **2016**.

5. Tian, C.; Cui, C.; Xu, L.; Gu, Y.; Sun, X. Dynamic strain aging in a newly developed Ni-Co-Base superalloy with low stacking fault energy. *J. Mater. Sci. Technol.* **2013**, *29*, 873–878.

6. Chatterjee, A.; Sharma, G.; Tewari, R.; Chakravartty, J.K. Investigation of the Dynamic Strain Aging and Mechanical Properties in Alloy-625 with Different Microstructures. *Metall. Mater. Trans. A* **2015**, *46*, 1097–1107.

7. Maj, P.; Zdunek, J.; Gizynski, M.; Mizera, J.; Kurzydlowski, K.J. Statistical analysis of the Portevin-Le Chatelier effect in Inconel 718 at high temperature. *Mater. Sci. Eng. A* **2014**.

8. American Society for Testing and Materials (ASTM) ASTM B443 - 00(2014) Standard Specification for Nickel-Chromium-Molybdenum-Columbium Alloy(UNS N06625) and Nickel-Chromium-Molybdenum-SiliconAlloy (UNS N06219) Plate, Sheet, and Strip 2014, 7.

9. American Society for Testing and Materials (ASTM) ASTM E139-11 Standard Test Methods for Conducting Creep, Creep Rupture, and Stress Rupture Tests of Metallic Materials 2011, 11.

10. American Society for Testing and Materials (ASTM) ASTM E112-13 Standard Test Methods for Determining Average Grain Size 2013, 28.

11. Hrutkay, K.; Kaoumi, D. Tensile deformation behavior of a nickel based superalloy at different temperatures. *Mater. Sci. Eng. A* **2014**, *599*, 196–203.

Preprints (www.preprints.org) | NOT PEER-REVIEWED | Posted: 31 December 2018 doi:10.20944/preprints201812.0359.v1

Peer-reviewed version available at Metals 2019, 9, 301; doi:10.3390/met9030301

12. Hale, C..; Rollings, W..; Weaver, M.. Activation energy calculations for discontinuous yielding in Inconel 718SPF. *Mater. Sci. Eng. A* **2001**, *300*, 153–164.

13. Rahman, M.S.; Priyadarshan, G.; Raja, K.S.; Nesbitt, C.; Misra, M. Characterization of high temperature deformation behavior of INCONEL 617. *Mech. Mater.* **2009**, *41*, 261–270.

14. Wright, J.K.; Carroll, L.J.; Cabet, C.; Lillo, T.M.; Benz, J.K.; Simpson, J.A.; Lloyd, W.R.; Chapman, J.A.; Wright, R.N. Characterization of elevated temperature properties of heat exchanger and steam generator alloys. *Nucl. Eng. Des.* **2012**, *251*, 252–260.

15. Fournier, L.; Delafosse, D.; Magnin, T. Oxidation induced intergranular cracking and Portevin-Le Chatelier effect in nickel base superalloy 718. *Mater. Sci. Eng. A* **2001**.

16. Kaoumi, D.; Hrutkay, K. Tensile deformation behavior and microstructure evolution of Ni-based superalloy 617. *J. Nucl. Mater.* **2014**.

17. Mo, K.; Lovicu, G.; Chen, X.; Tung, H.M.; Hansen, J.B.; Stubbins, J.F. Mechanism of plastic deformation of a Ni-based superalloy for VHTR applications. *J. Nucl. Mater.* **2013**.

18. Nalawade, S.A.; Sundararaman, M.; Kishore, R.; Shah, J.G. The influence of aging on the serrated yielding phenomena in a nickel-base superalloy. *Scr. Mater.* **2008**, *59*, 991–994.

19. Lee, K.O.; Lee, S.B. Modeling of materials behavior at various temperatures of hot isostatically pressed superalloys. *Mater. Sci. Eng. A* **2012**, *541*, 81–87.

20. Cottrell, A.H. LXXXVI. A note on the Portevin-Le Chatelier effect. *London, Edinburgh, Dublin Philos. Mag. J. Sci.* **1953**, *44*, 829–832.

21. Nagesha, A.; Goyal, S.; Nandagopal, M.; Parameswaran, P.; Sandhya, R.; Mathew, M.D.; Mannan, S.K. Dynamic strain ageing in Inconel®Alloy 783 under tension and low cycle fatigue. *Mater. Sci. Eng. A* **2012**.

22. Sleeswyk, A.W. Slow strain-hardening of ingot iron. *Acta Metall.* **1958**.

23. Cuddy, L..; Leslie, W.C. Some aspects of serrated yielding in substitutional solid solutions of iron. *Acta Metall.* **1972**, *20*, 1157–1167.

24. Cheng, J.; Nemat-Nasser, S. Model for experimentally-observed high-strain-rate dynamic strain aging in titanium. *Acta Mater.* **2000**.

25. van Liempt, P.; Onink, M.; Bodin, A. Modelling the Influence of Dynamic Strain Ageing on Deformation Behaviour. *Adv. Eng. Mater.* **2002**, *4*, 225–232.

26. McCormigk, P.G. A model for the Portevin-Le Chatelier effect in substitutional alloys. *Acta Metall.* **1972**.

27. van den Beukel, A. Theory of the effect of dynamic strain aging on mechanical properties. *Phys. Status Solidi* **1975**, *30*, 197–206.

Preprints (www.preprints.org) | NOT PEER-REVIEWED | Posted: 31 December 2018 doi:10.20944/preprints201812.0359.v1

Peer-reviewed version available at Metals 2019, 9, 301; doi:10.3390/met9030301

28. Wycliffe, P.; Kocks, U.F.; Embury, J.D. On dynamic and static ageing in substitutional and interstitial alloys. *Scr. Metall.* **1980**, *14*, 1349–1354.

29. Van Den Beukel, A.; Kocks, U.F. The strain dependence of static and dynamic strain-aging. *Acta Metall.* **1982**, *30*, 1027–1034.

30. Estrin, Y.; McCormick, P.G. Modelling the transient flow behaviour of dynamic strain ageing materials. *Acta Metall. Mater.* **1991**.

31. Estrin, Y. A versatile unified constitutive model based on dislocation density evolution. In *High temperature constitutive modeling: theory and application*; Freed, A.D., Walker, K.P., Eds.; American Society of Mechanical Engineers: New York, 1991; pp. 65–83.

32. Schlipf, J. Dislocation dynamics in strain aging alloys. *Acta Metall. Mater.* **1992**, *40*, 2075–2084.

33. Gilat, A.; Wu, X. Plastic deformation of 1020 steel over a wide range of strain rates and temperatures. *Int. J. Plast.* **1997**, *13*, 611–632.

34. Rodriguez, P. Serrated plastic flow. *Bull. Mater. Sci.* **1984**, *6*, 653–663.

35. Rodriguez, P.; Venkadesan, S. Serrated Plastic Flow Revisited. *Solid State Phenom.* **1995**, *42–43*, 257–266.

36. Evans, R.W.; Wilshire, B. *Introduction to creep*; The Institute of Materials: London, England, 1993;

37. Ashby, M.F.; Frost, H.J. *Deformation-mechanism Maps: The Plasticity and Creep of Metals and Ceramics*; Pergamon Press: Oxford, 1982;

38. Moore, I.J.; Taylor, J.I.; Tracy, M.W.; Burke, M.G.; Palmiere, E.J. Grain coarsening behaviour of solution annealed Alloy 625 between 600–800 °C. *Mater. Sci. Eng. A* **2017**, *682*, 402–409.